Bull. Mater. Sci., Vol. 30, No. 4, August 2007, pp. 339–344. © Indian Academy of Sciences.

Thermal decomposition of natural dolomite

S GUNASEKARAN[†] and G ANBALAGAN*

PG and Research Department of Physics, Presidency College, Chennai 600 005, India
[†]PG and Research Department of Physics, Pachaiyappa's College, Chennai 600 030, India

MS received 3 November 2006; revised 22 May 2007

Abstract. Thermal decomposition behaviour of dolomite sample has been studied by thermogravimetric (TG) measurements. Differential thermal analysis (DTA) curve of dolomite shows two peaks at 777·8°C and 834°C. The two endothermic peaks observed in dolomite are essentially due to decarbonation of dolomite and calcite, respectively. The TG data of the decomposition steps have also been analysed using various differential, difference-differential and integral methods, viz. Freeman–Carroll, Horowitz–Metzger, Coats–Redfern methods. Values of activation entropy, Arrhenius factor, and order of reaction have been approximated and compared. Measured activation energies vary between 97 and 147 kJ mol^{-1}. The large fluctuation in activation energy is attributed to the presence of impurities such as SiO_2, Al_2O_3, Fe_2O_3, Cl^- etc in the samples. FTIR and XRD analyses confirm the decomposition reaction. SEM observation of the heat-treated samples at 950°C shows cluster of grains, indicating the structural transformation.

Keywords. TGA–DTA; FTIR; X-ray diffraction; dolomite.

1. Introduction

Dolomite typically occurs as the major constituent of sedimentary formations in association with calcite. Thermal analysis might offer the means of defining the fraction of each mineral lattice in such mixtures and the concentration of each cation in each lattice. The correlation of the thermal data with the structural pattern should provide a broader understanding of these minerals in their natural occurrence. Romero Salvador *et al* (1989) studied the effects of experimental variables i.e. sample weight, particle size, purge gas velocity and crystalline structure, on the kinetic parameters of calcium carbonate decomposition. Criado and Ortega (1992) studied the influence of particle size on the thermal decomposition of calcium carbonate and found that the activation energy of thermal decomposition of calcium carbonate smoothly increases as the particle size increases. This behaviour can be attributed to the lower particle size and greater fraction of $CaCO_3$ molecules located on surface with regard to the bulk. Therefore, the activation energy decreases because of the extra calcium carbonate stored on the surface of the smaller particles. In general, it has been reported that a diminition of the activation energy takes place when the sample size increases. This behaviour would be attributed to the influence of heat and mass transfer effects because of the poor control that is usually exerted on both decomposition rate (i.e. rate of heat evolution) and pressure of the environment. Many researchers have studied the kinetics of thermal decomposition of carbonate minerals (Powell and Searcy 1980; Warne *et al* 1981; Iwafuchi *et al* 1983; Borgwardt 1985; Yariv 1989; McInosh *et al* 1990; Rubiera *et al* 1991; McCauley and Johnson 1991; Mulokozi and Lugwisha 1992; Ersoy-Merichoyu *et al* 1993; Shoval *et al* 1993; Xiao *et al* 1997). A general review of the literature on the decomposition of carbonates indicates that a great deal of variability exists in the reported values of the decomposition temperatures, activation energies and rates of decomposition. Although the decomposition of NBS dolomite sample has been reported (Criado and Ortega 1991), there have been no systematic studies on dolomite samples having a small concentration of naturally occurring alkali earth salts. In this paper, the effect of chlorine ions on the decomposition kinetics of dolomite at various temperatures studied by differential thermal analysis, thermogravimetric analysis, Fourier transform infrared spectroscopy and powder X-ray diffraction, have been reported.

2. Experimental

Natural dolomite sample collected from Neralakere mines, Bagalkot area of (latitude, 16°11′, longitude, 75°45′) Karnataka state was ground with agate mortar and pestle. The powder sample with size, 1·2 nm, was subjected to X-ray diffraction (XRD), Fourier-transform infrared spectroscopy (FT–IR) and thermal analyses (differential thermal analysis (DTA) and thermogravimetric analysis (TGA)).

*Author for correspondence (anbu24663@yahoo.co.in)

The particle size was determined using the Scherrer formula (Kunel *et al* 1997).

XRD analysis was performed with a SEIFERT X-ray diffractometer with CuKα radiation (λ = 1·54 Å), Cu filter on secondary optics, 45 kV power and 20 mA current. The powder sample was mounted on a quartz support to minimize background.

Perkin-Elmer spectrum one FT–IR spectrometer was used, and the samples were analysed in KBr pellets. Spectra were traced in the range 4000–400 cm^{-1}, and the band intensities were expressed in transmittance (%). The infrared analysis helped in the identification of the main groups in the carbonate samples.

The powder sample was heated in a muffle furnace under air atmosphere for 6 h in each temperature. The spectral recordings were carried out at room temperature.

Thermal analysis was performed in a simultaneous TG–DTA (Netzsch STA 409). The experimental conditions were: (i) continuous heating from room temperature to 1000°C at a heating rate of 10 K/min, (ii) N_2-gas dynamic atmosphere (90 cm^3 min^{-1}), (iii) alumina, as reference material and (iv) sample: 53·37 mg of the sample having grain size 1·2 nm without pressing. The temperature was detected with a Pt–Pt 13% Rh thermocouple fixed in a position near the sample pan. TG and DTA curves were obtained. The following data was obtained by thermal analysis: (i) reaction peak temperature and main effect (endothermic or exothermic) and (ii) content of bound water, which is the weight loss in the temperature range 200–600°C and content of CO_2 released during the decomposition of carbonate phases.

3. Results and discussion

Table 1 gives composition of the sample, which was determined by the standard analysis (Vogel 1951). The main undesirable impurities in the carbonate rocks are silica, K_2O, Na_2O, Cl^- and alumina. These impurities combine with calcium oxide at elevated temperatures to form a slag, which reduce the pore volume and the amount of available active lime (Chan *et al* 1970). Such impurities either occurred in the matrix or came from the material in the crevices and other strata excavated along with limestone. Samples were chosen from quarries in which these impurities were low.

3.1 *Differential thermal analysis*

The typical DTA curve of dolomite sample is presented in figure 1. The thermal curves representing the carbonate mineral are characterized by endothermic peaks at various temperatures caused by the evolution of carbon dioxide (figure 1). DTA curve of dolomite shows two endotherms at 772·6°C and 834°C. The first one begins at 687°C, reaches a peak at 773°C and ends at 781°C and the second one begins at 781°C, reaches a peak at 834°C and ends at 916°C. The lower temperature peak represents the decomposition of the dolomite structure, releasing carbon dioxide from the carbonate ion associated with magnesium part of the structure accompanied by the formation of calcite and magnesium oxide. The higher temperature peak represents the decomposition of calcite with the evolution of carbon dioxide (McInosh *et al* 1990). Mc Cauley and Johnson (1999) observed the peak temperatures at 790°C and 845°C for +16 mesh dolomite samples. However, Li and Messing (1983) reported the corresponding peak temperatures for $CaCl_2$ doped dolomite sample at 750°C and 830°C. This result suggests that the presence of salt (Cl^-) enhances the decomposition of dolomite in the present study. The decomposition process is initiated at lower temperatures than observed for the pure dolomite. The salts promote the formation of MgO and $CaCO_3$ during the early stage of decomposition. The ratio of the peak area (~5·2) and the high characteristic temperature (773°C) indicates that the dolomite is in well-ordered crystalline structure (Garn 1965), which is also confirmed through X-ray diffraction analysis. According to Barcina *et al* (1997), smaller size of magnesium with respect to calcium facilitates the magnesium mobility and thus the formation of carbon dioxide associated to magnesium oxide is kinetically favoured against the formation of CO_2 associated to calcium oxide. The first endothermic peak of dolomite, however, caused by the reaction of more complicated mechanism, has inverted symmetry/shape index of 1·45 (Garn 1965). After calcinations, the resultant oxides have lower molar volumes, larger surface areas, and greater porosities than the carbonates. The calcination of a carbonate entails the formation of an oxide having a pseudo-lattice of the carbonate and subsequent recrystallization to the normal cubic lattice of the oxide. If the temperature is high enough, sintering of oxide takes place (Glasson 1958). The results indicate that the effect of Fe_2O_3 and Al_2O_3 on peak temperature is maximum when these oxides are present in low concentrations.

3.2 *Thermogravimetric analysis*

The typical TG curve of dolomite sample is presented in figure 1. The observed weight loss was 1·33% below

Table 1. Results of the chemical analysis of samples (%).

Sample code	CaO	MgO	SiO_2	Fe_2O_3	Al_2O_3	K_2O	Na_2O	Cl^-	LOI
D_{01}	30·24	21·33	0·18	0·63	0·25	0·03	0·23	0·19	46·04

Table 2. Kinetic parameters for the thermal decomposition of dolomite in N_2 atmosphere for different calculation methods.

	Freeman–Carroll			Coats–Redfern					Horowitz–Metzger		
Sample code	E (kJ mol^{-1})	Log A (s^{-1})	S (JK mol^{-1})	E (kJ mol^{-1})	Log A (s^{-1})	S (JK mol^{-1})	n	r	E (kJ mol^{-1})	Log A (s^{-1})	S (JK mol^{-1})
D_{01}	113·56	3·246	−133·586	123·684	3·743	−183·851	0·15	0·991	147·58	4·346	−172·55

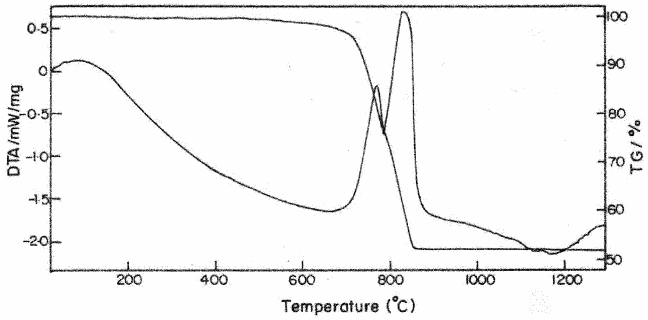

Figure 1. TG–DTA curves of dolomite.

600°C and between 600°C and 850°C, it was 46·6%. The weight loss detected in the temperature range 100–120°C, was followed by a weight loss attributed to the decomposition of carbonates. The weight loss in this temperature range can be attributed to the chemically bound water. The kinetics of decomposition processes were analysed by means of the three popular methods (Freeman and Carroll 1958; Coats and Redfern 1964; Horowitz and Metzger 1963). Measured activation energies are given in table 2 and are in agreement with that reported by Criado and Ortega (1991) for pure dolomite sample. The measured activation energy indicates that Cl^- do not activate the process by lowering the thermal requirements for decomposition. The slight variation in activation energy may be attributed to the difference in particle size and mineral origin in the samples. Lower the particle size, greater the fraction of molecules located on the surface with regard to the bulk. The wide dispersion of the available data is in relation to the influence of physical processes, viz. inter- and intra-particle diffusion, heat transfer resistance, sintering etc. Garcia Calvo *et al* (1990) studied the influence of macro-kinetic parameters on the value of the activation energy over a wide range of experimental conditions and concluded that the influence of macro-kinetic parameter is low within this range. The calculated activation energy, E, increases with increasing concentration of the decomposition product (CO_2), which is similar to the observation of Ersoy-Merichoyu *et al* (1993). This change is attributed to the reversible nature of the decomposition reaction. The increase in E is balanced by a corresponding increase in A which is due to the compensation behaviour. If higher activation energies are obtained, the pre-exponential factors (A) are higher too. The

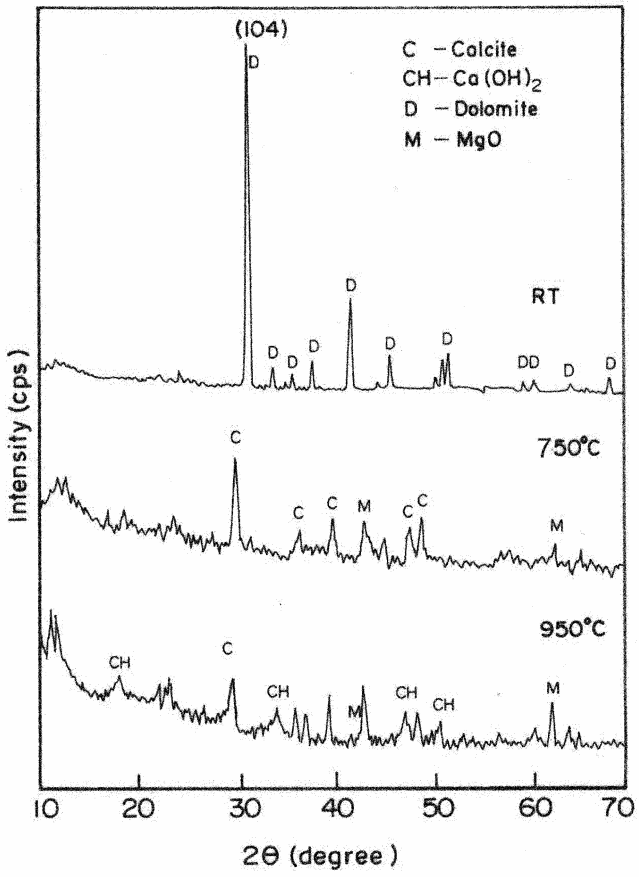

Figure 2. XRD pattern of dolomite at different temperatures.

observed kinetic parameters were found to be strongly affected by small amounts of impurities; however, the kinetic model is not affected. Comparison of the values of E and A in the present study with those values of pure calcite reported by Garcia Calvo *et al* (1990) indicates that the presence of impurities is a cause of variation of kinetic parameters obtained. The impurities could function as catalysts owing to their influence in the crystalline structure.

3.3 *X-ray diffraction analysis*

Figure 2 depicts the powder X-ray diffraction pattern of natural dolomite sample at different temperatures. The room temperature XRD pattern of the sample displays

Table 3. Indexed powder XRD pattern for natural dolomite.

Sl. no.	h	k	l	d (Å) obs	d (Å) cal	Diff. D (Å)	2θ (degree) obs	2θ (degree) cal	Diff. 2θ (degree)
1	0	1	2	3·6917	3·6906	0·0011	24·087	24·094	–0·007
2	1	0	4	2·8884	2·8887	–0·0003	30·935	30·931	0·004
3	0	0	6	2·6720	2·6724	–0·0004	33·511	33·506	0·005
4	0	1	5	2·5417	2·5408	0·0009	35·283	35·296	–0·013
5	1	1	0	2·4100	2·4104	–0·0004	37·281	37·275	0·006
6	1	1	3	2·1974	2·1975	–0·0001	41·042	41·040	0·002
7	0	2	1	2·0209	2·0214	–0·0005	44·812	44·801	0·011
8	0	2	4	1·8519	1·8522	–0·0003	49·158	49·150	0·008
9	0	1	8	1·8095	1·8098	–0·0003	50·390	50·380	0·010
10	1	1	6	1·7920	1·7919	0·0001	50·918	50·919	–0·001
11	2	1	1	1·5722	1·5726	–0·0004	58·676	58·659	0·017
12	1	2	2	1·5493	1·5495	–0·0002	59·628	59·620	0·008
13	2	1	4	1·4698	1·4698	0·0000	63·214	63·214	0·000
14	0	3	0	1·3933	1·3934	–0·00008	67·126	67·121	0·005

Table 4. Unit cell parameters of natural dolomite at different temperatures.

Temperature (°C)	a (Å)	c (Å)	c/a (Å)	Volume (Å)^3
RT	4·8247	15·9680	3·3135	322·28
650	4·9680	17·1008	3·4422	365·5
750	5·0103	17·0146	3·3959	369·9
850	5·0466	16·9380	3·3563	373·6
950	5·0348	16·9558	3·3671	372·2

Table 5. FWHM of principal reflections of dolomite for different heat treatments.

	Dolomite	
Temperature (°C)	(104)	(202)
650	0·16	0·24
750	0·16	0·24
850	0·16	0·12
950	0·16	0·16

Table 6. Observed X-ray data for the heat treated dolomite sample (750°C) and reported data for calcite.

	d (Å) for calcite			
(h k l)	Observed	Reported	JCPDS Card 5-586	Intensity
(0 1 2)	3·8409	3·8520	3·80	12
(1 0 4)	3·0334	3·0300	3·035	100
(0 0 6)	2·8889	2·8340	2·845	3
(1 1 0)	2·4993	2·4950	2·495	14
(1 1 3)	2·2877	2·2840	2·285	18
(2 0 2)	2·1084	2·0940	2·095	18
(0 2 4)	1·9179	1·9260	–	–
(1 1 6)	1·8837	1·8750	1·875	17
(2 1 5)	1·4968	1·4730	1·473	2

ASTM card no. (24-274).

Table 7. Vibrational frequency assignments (FT–IR).

ν_1 (cm^{-1})	ν_2 (cm^{-1})	ν_3 (cm^{-1})	ν_4 (cm^{-1})	$\nu_1 + \nu_4$ (cm^{-1})	$2\nu_2 + \nu_4$ (cm^{-1})
–	881	1446	726	1881	2525

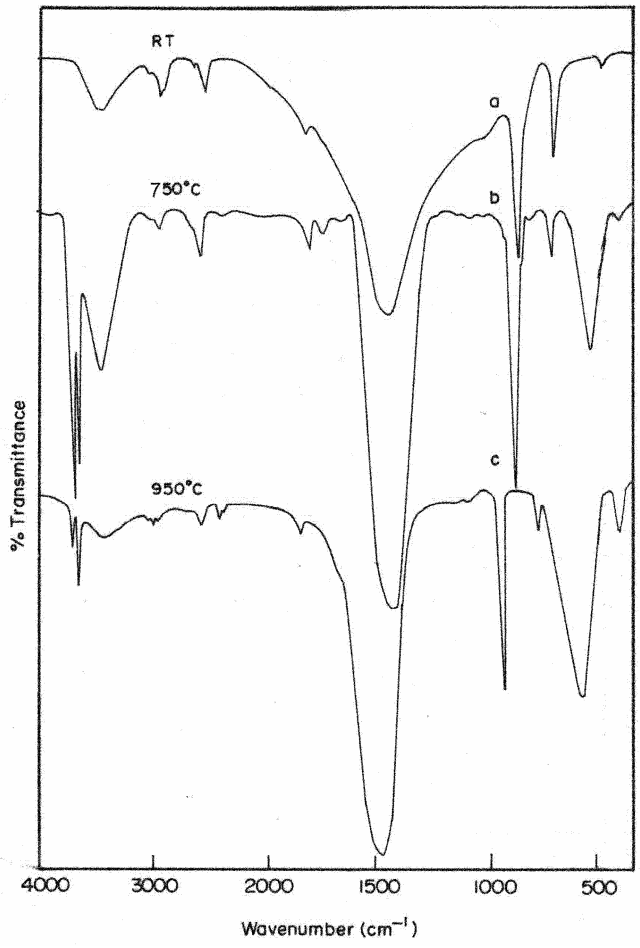

Figure 3. FTIR spectra of dolomite at different temperatures.

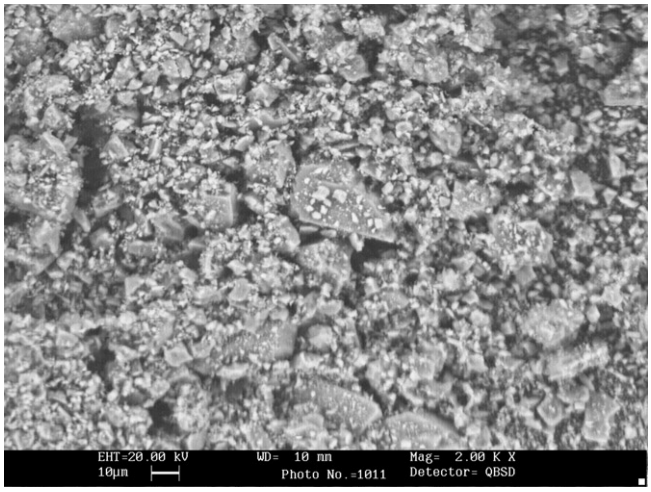

Figure 4. SEM photograph of dolomite at room temperature.

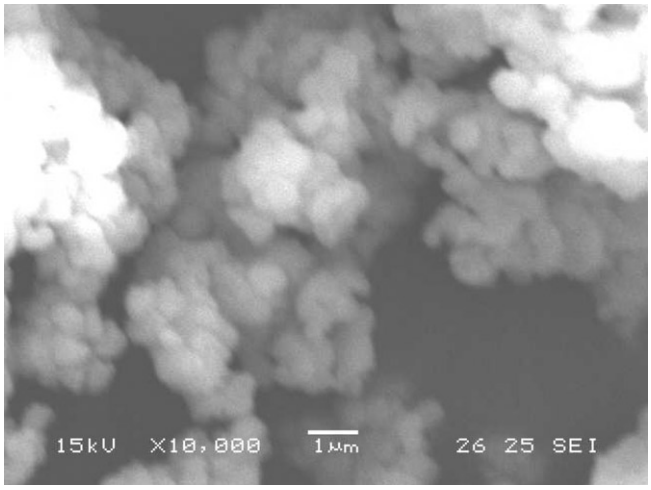

Figure 5. SEM photograph of dolomite at 950°C.

sharp diffractions that can be attributed to dolomite (JCPDS Files card 11-78; 1999). Table 3 gives various Bragg reflections that are indexed using JCPDS Files card 11-78 and the calculated unit cell dimensions of natural dolomite at different temperatures are compiled in table 4. In table 5, FWHM of (104) and (202) reflections of dolomite are compared for different heat treatments. It can be noticed that the general pattern remains the same and in addition, there is no change in the FWHM of the (104) reflection. However, the (202) reflection shows slight decrease in the FWHM value. The original reflection disappeared completely and new lines are developed at the asymmetric positions of (104) and (202) reflections. In table 6, the *d* spacing of the reflections observed for 750°C heat treatment is compared with those reported in the literature for calcite indicating that the crystal structure of dolomite has been transformed completely to calcite structure during heat treatment.

3.4 *FTIR spectral analysis*

The typical transmittance FTIR spectra of the dolomite mineral are shown in figure 3. In the room temperature FTIR spectra of the samples, the out-of-plane bending (ν_2), the asymmetric stretching (ν_3), and the in-plane bending (ν_4) modes of the carbonate group are found to be active. Besides the internal modes, the $\nu_2 + \nu_4$ combination mode has also been observed (Adler and Kerr 1963; White 1974; Legodi *et al* 2001) and the observed bands are compiled in table 7. Additionally peaks due to silicates (1088 cm^{-1}) and H-bonded water (at 3400 cm^{-1}) are visible (Keeling 1963). In addition, the weak band due to quartz (465 cm^{-1}) is also visible. The characteristic dolomite bands are shifted to 713, 876 and 420 cm^{-1} in the FTIR spectra of 750°C heat-treated dolomite sample (figure 3). This clearly indicates the structural transformation of dolomite to calcite. At this stage, a strong and broad band at 540 cm^{-1} due to magnesium oxide is also visible. At 950°C, the 1420 cm^{-1} band shifted to 1413 cm^{-1} and the intensity of the band, 713 cm^{-1}, very much decreased. SEM microphotographs of the heat-treated and untreated samples are shown in figures 4 and 5. SEM microphotograph of the untreated samples shows distinct grains, however, the heat-treated (950°C) samples exhibit clusters of grains confirming the thermal decomposition.

4. Conclusions

DTA curve of dolomite shows two peaks at 777·8°C and 834°C. The two-stage decomposition reaction is confirmed by FTIR and XRD analysis. At 750°C, the dolomite structure is changed into calcite, which is confirmed by the presence of calcite characteristic peaks in the FTIR spectra at 713, 875 and 1420 cm^{-1}. The presence of characteristic reflections at 3·0334 and 2·4993 Å for calcite and MgO, respectively also confirm the first stage decomposition of dolomite. At 950°C, the thermal decomposition reaction is completed which is confirmed by FTIR and XRD analysis. The large fluctuation in the observed activation energies is due to the presence of impurities in the samples. The impurities could function as catalysts owing to their influence in the crystalline structure. The results show that the clay with which they are heated which is reflected by the differences in the activation energy, affects dolomite decomposition. These results could be important in site consideration of the dolomite sample.

References

Adler H H and Kerr P F 1963 *Am. Mineral.* **48** 839

Barcina L M, Espina A, Suarez M, Garcia J R and Rodriguez J 1997 *Thermochim. Acta* **290** 181

Borgwardt R H 1985 *AIchE* **31** 103

Chan R K, Murthi K S and Harrison D 1970 *Can. J. Chem.* **48** 2972

Coats A W and Redfern J P 1964 *Nature* (*London*) **201** 68
Criado J M and Ortega A 1991 *J. Thermal Anal. & Calorimetry* **37** 2369
Criado J M and Ortega A 1992 *Thermochim Acta* **195** 163
Ersoy-Merichoyu A, Kuchkbayrak S and Durus B 1993 *J. Thermal Anal*. **39** 707
Freeman E S and Carroll B 1958 *J. Phys. Chem*. **62** 394
Garcia Calvo E, Arranz M A and Leton P 1990 *Thermochim. Acta* **170** 7
Garn D D 1965 *Thermoanalytical methods of investigation* (New York: Academic Press)
Glasson D R 1958 *J. Appl. Chem*. **8** 793
Horowitz H H and Metzger G 1963 *Anal. Chem*. **35** 1464
Iwafuchi K, Watanabe C and Otsuka R 1983 *Thermochim. Acta* **66** 105
JCPDS Files card 5-586 and 11-78 1999
Keeling P S 1963 *Trans. Br. Ceram. Soc*. (*GB*) **62** 549
Kunel D, Modi and Jadhav K M 1997 *Indian J. Pure & Appl. Phys*. **25** 594
Legodi M A, deWaal D and Potgieter J H 2001 *Appl. Spectrosc*. **55** 361
Li Mao Qiang and Messing G L 1984 *Thermochim Acta* **78** 9
Mc Cauley R A and Johnson L A 1991 *Thermochim. Acta* **185** 27
McInosh L M, Sharp J H and Willburn F W 1990 *Thermochim. Acta* **165** 281
Mulokozi A M and Lugwisha E 1992 *Thermochim. Acta* **194** 375
Powell E K and Searcy A W 1980 *Metall. Trans*. **B11** 427
Romero Salvador A, Garcia Calvo E and Beneitz Aparico M 1989 *Thermochim. Acta* **143** 339
Rubiera F, Fuertes A B, Pis J J, Artos V and Marban G 1991 *Thermochim. Acta* **179** 125
Shoval S, Gaft M, Beck P and Krish V 1993 *J. Thermal Anal*. **40** 263
Vogel A I 1951 *Quantitative inorganic analysis* (London: Longmans) p. 582
Warne S S J, Morgan D J and Milondowshi A E 1981 *Thermochim. Acta* **51** 105
White W B 1974 *Min. Soc. Monogr*. **4** 227
Xiao K, Sichen D U, Sohn H Y and Seetharaman S 1997 *Metall. and Mater. Trans*. **B28** 1157
Yariv Shmuel 1989 *Thermochim. Acta* **148** 421